DEPARTMENT OF PHYSICS, UNIVERSITY OF JYVÄSKYLÄ
RESEARCH REPORT No. 3/1998

BETA-DECAY STUDIES OF HIGH-ISOSPIN NUCLEI ^{31}Ar, ^{33}Ar AND ^{41}Ti

BY
ANTTI HONKANEN

Academic Dissertation
for the Degree of
Doctor of Philosophy

Jyväskylä, Finland
February 1998

URN:ISBN:978-951-39-9092-3
ISBN 978-951-39-9092-3 (PDF)
ISSN 0075-465X

Jyväskylän yliopisto, 2022

ISBN 951-39-0170-X
ISSN 0075-465X
KOPIJYVÄ OY – Jyväskylä 1998

DEPARTMENT OF PHYSICS, UNIVERSITY OF JYVÄSKYLÄ
RESEARCH REPORT No. 3/1998

BETA-DECAY STUDIES OF HIGH-ISOSPIN NUCLEI ^{31}Ar, ^{33}Ar AND ^{41}Ti

BY
ANTTI HONKANEN

Academic Dissertation
for the Degree of
Doctor of Philosophy

To be presented, by permission of the
Faculty of Mathematics and Natural Sciences
of the University of Jyväskylä,
for public examination in Auditorium FYS-1 of the
University of Jyväskylä on February 20, 1998,
at 12 o'clock noon

Jyväskylä, Finland
February 1998

Preface

Studies of this thesis have been carried out during the years 1994-1997 at Accelerator Laboratory of University of Jyväskylä (JYFL), at van de Graaf accelerator of University of Helsinki and at European Laboratory of Particle Physics (CERN). A detector telescope was developed for studies of this thesis. The possibility for testing the detector system in Helsinki was significant. Department of Physics in Jyväskylä has been a pleasant place to work. I am thankful to the whole Department of Physics for excellent working conditions and encouraging atmosphere.

Countless number of measurement shifts during the years have shown me the importance of group work. The IGISOL group has been a great team to work with. I would like to thank all the group members. Special thanks are addressed to my supervisor professor Juha Äystö, who inspiringly conducts the team. Also, I would like to thank Dr. Ari Jokinen, Mr. Markku Oinonen and Mr. Kari Peräjärvi with whom I have mainly been working together.

Professor Pertti Lipas, even as emeritus, has strongly been participating in the publications of this work by providing shell model calculations. He was also an outstanding character in revising the manuscripts of two of the publications. As an experimentalist I wish to express my gratitude to him for teaching and guiding me in the theoretical aspects. Special thanks belong also to Mr.Teemu Siiskonen for providing shell model calculations for this thesis.

As a member of international collaboration growded with distinguished senior scientists, I have been privileged to obtain extensive guidance and outlook of the field of experimental nuclear physics. The list of the people I would like to thank for successful collaboration and fruitful discussions is long. Therefore, I am assigning my gratitude to all collaborators of ISOL339 experiment at CERN, Madrid, Gothenburg and Aarhus.

Finally, I would like to thank my family for their support during the years. My warmest thanks are addressed to my son Pauli and to my wife Leena for their patience and inventive encouragement.

Jyväskylä, January 1998

Antti Honkanen

Abstract

This thesis is a review of five different articles already published or submitted for publication. Beta decay properties of proton-rich isotopes of ^{31}Ar, ^{33}Ar and ^{41}Ti were surveyed experimentally. In addition, the mechanism of beta-delayed two-proton emission was studied in the decay of ^{31}Ar. Two types of on-line mass separators were applied to select and transport the studied nuclei. The detection of delayed radiation was done by means of silicon, gas, germanium and scintillation detectors. A special construction of a gas-silicon detector telescope was developed for these studies. In comparison with conventional silicon telescopes the new telescope proves to be progressive. It allows detection of charged particles with better energy resolution and reduced detection threshold.

All the studied nuclei are beta-delayed proton precursors. They possess high beta-decay energies, which allowed measurement of beta-decay strength up to 8 MeV excitation in ^{41}Sc and 14 MeV in ^{31}Cl. Fifteen new energy levels were discovered in ^{31}Cl. Isospin impurity in the lowest $J^{\pi}=3/2^{+}$, $T=3/2$ level in ^{41}Sc was deduced to be $\approx 10\%$. Partial decay widths for proton emission were studied for ^{33}Ar. Comparison of experimental results to output of the shell model calculations showed the generally acknowledged problems, such as, quenching of the beta strength and scarcity in predicting level energies. A conclusion cannot be given for the mechanism of 2p-emission in the decay of ^{31}Ar.

Contents

1. Introduction

Beta decay is a process of weak interaction and provides an excellent probe to study fundamental phenomena by means of low energy nuclear physics. Together with alpha decay it constitutes a major mode of radioactive processes. As a weak interaction process beta decay is characterized by relatively long time scales. Half lives of beta decaying nuclides vary from milliseconds up to 10^{24} years. Energy release in known beta decays vary from 18.6 keV (^{3}H, β^-) up to 22 800 keV (^{22}N, β^-) [1].

In this thesis beta-decay strength and delayed proton emissions of proton-rich high-isospin nuclei are studied. The nuclei studied: ^{31,33}Ar and ^{41}Ti are located in the sd-shell or in the crossing region of sd- and fp-shells. Experimental transition probabilities are compared to theoretical ones calculated with a standard shell model. In these shell model calculations two different computer programs [2] and two different interactions were used. The results of the beta decay measurements can be used as tests for the large scale shell model calculations.

Astrophysical processes are responsible for the existence of a large fraction of elements. Measurements of decay properties, such as half-lives, binding energies, energies of excited states and their widths are essential in improving our knowledge on astrophysical processes. The rp-process path goes through the region of nuclides with M_T<0 in the sd-shell.

Beta decay studies at the sd-shell are also interesting from the point of view of the standard solar model [3]. An inverse beta-decay (neutrino capture) is applied in neutrino detectors. The detection medium of those detectors consists of stable isotopes, whose beta-decay properties are not possible to measure directly. Therefore, the beta decay strength leading to ν-capture cross sections is obtained from the decay strength of a mirror nucleus by applying the charge symmetry of nuclear force. The earliest attempt to detect solar neutrinos was the application of neutrino capture of ^{37}Cl to ^{37}Ar [3], where the decay strength can be studied by measuring the beta decay of ^{37}Ca. Recently a proposal [4] to detect neutrino capture: $\nu_e + {}^{40}\mathrm{Ar} \rightarrow {}^{40}\mathrm{K} + e^-$ has been made. The mirror decay in the latter case is $^{40}\mathrm{Ti} \rightarrow {}^{40}\mathrm{Sc} + e^+ + \nu_e$. The study of ^{41}Ti pave the way to a high-resolution measurement of ^{40}Ti.

Pairing of nucleons in the nucleus is a known feature. Beta-delayed deuteron emission has been detected from the 2n-halo state in ^{11}Li [5]. The existence of such a Borromean system indicates strong correlation between the paired nucleons. So far, there is no observation of similar beta-delayed process from a proton rich nucleus. In addition, no observation of a direct ground state emission of two protons has been done. The direct emission has been proposed to be manifested by correlated simultaneous emission of two protons [6]. The cluster of two protons, ^{2}He is expected to be the origin of hydrogen burning in stars and therefore the starting point of all of A>1 nuclei. The radiative two-proton capture is one of the discussed tasks in rapid-proton capture process (rp) studies [7] and can be considered as a reverse reaction to the sequential emission of two protons. The information of the two-proton emission, thus, has importance in astrophysics as well.

Decay of proton-rich, high-isospin nuclei is characterised by the emission of charged particles due to the reasons discussed in Chapter 2. The decay of ^{33}Ar has earlier been studied by Hardy et al. [8] and Borge et al.[9], who deduced the Gamow-Teller strength distribution and by Schardt and Riisager [10], who extracted the GT-strength to the Isobaric Analog State (IAS) by measuring the broadening in the proton peak.

Several experiments at GANIL have identified the main decay branches of ^{31}Ar and determined the accuarte half-life [11]. However, these experiments suffered from modest energy resolution and contamination of ^{29}S. The first experiment at CERN was made for the search of direct 2p-emission [12].

Sextro et. al have studied the decay of ^{41}Ti using He-Jet technique [13]. They deduced beta-decay distribution and half-life for the decay of ^{41}Ti. Zhou et al. measured several additional proton transitions also using He-Jet technique [14]. In this work the first results measured using a mass-separeted source of ^{41}Ti are given.

Experimentally the main emphasis was put on the detection of single or higher multiplicity protons. A special detector telescope was designed for this purpose. It consists of a thin gas filled detector and of a silicon detector. Especially in studies for beta-delayed charge particle precursors such a telescope has proven to be very useful [15].

In the concluding chapter the systematics of isospin mixing and the quenching of the beta-decay in some "upper sd-shell" nuclides are compiled based on the results of the enclosed papers and

earlier publications. The complete results of the experiments and detailed descriptions of them are published in the enclosed articles listed below:

1. ***Gas-silicon detector telescope for charged particle spectroscopy***
A. Honkanen, M. Oinonen, K. Eskola, A. Jokinen, J. Äystö, the ISOLDE collaboration, Nuclear Instruments and Methods in Physics Research **A 395** (1997) 217.

2. ***Fine structure in the beta-delayed proton decay of ^{33}Ar***
A. Honkanen, L. Axelsson, J. Äystö, M.J.G. Borge, B. Jonson, A. Jokinen, I. Martel, G. Martínez-Pinedo, I. Mukha, T. Nilsson, G. Nyman, B. Petersen, A. Poves, M.H. Smedberg,A. Teijeiro, O. Tengblad, the ISOLDE Collaboration, Nuclear Physics **A 611** (1996) 47.

3. ***High-resolution study of the beta decay of ^{41}Ti***
A. Honkanen, P. Dendooven, M. Huhta, G. Lhersonneau, P.O. Lipas, M. Oinonen, J.-M. Parmonen, H. Penttilä, K. Peräjärvi, T. Siiskonen, J. Äystö, Nuclear Physics **A 621** (1997) 689.

4. ***Beta decay of ^{31}Ar***
L. Axelsson, J. Äystö, M.J.G. Borge, L.M. Fraile, H.O.U. Fynbo, A. Honkanen, P. Hornshøj, A. Jokinen, B. Jonson, P.O. Lipas, I. Martel, I. Mukha, T. Nilsson, G. Nyman, B. Petersen, K. Riisager, M.H. Smedberg, O. Tengblad, the ISOLDE collaboration. Submitted to Nuclear Physics A.

5. ***Two-proton emission in the decay of ^{31}Ar***
L. Axelsson, J. Äystö, U.C. Bergman, M.J.G. Borge, L.M. Fraile, H.O.U. Fynbo, A. Honkanen, P. Hornshøj, A. Jokinen, B. Jonson, I. Martel, I. Mukha, T. Nilsson, G. Nyman, B. Petersen, K. Riisager, M.H. Smedberg, O. Tengblad and the ISOLDE collaboration, Nuclear Physics A, in press.

In the enclosed articles [Publ.1,2,3,4] the author of this thesis has been responsible for the experimental parts by sharing in setting up the detectors and the electronics, analysing and interpreting the data and in writing the publications. In [Publ.5] the interpretation of the experimental data and writing the publication has been done by other contributors.

Errata

Publication 2. *Fine structure in the beta-delayed proton decay of ^{33}Ar*

In page 53. the squared matrix element describing the transition probability of a proton decay from $3/2^+$ states in ^{33}Cl should be written as:

$$|\langle {}^{33}Cl(3/2^+)\ |a_j^\dagger|{}^{32}S(J_f)_n\rangle|^2 \qquad \textbf{(1)}$$

Publication 3. *High-resolution study of the beta decay of ^{41}Ti*

In Table 2. the energy of 4644(5) keV should be 4653(12) keV

2. Beta decay of proton-rich nuclei

Beta decay offers a possibility to obtain information on weakly produced nuclei far off the valley of the stability. Other spectroscopic methods, such as reaction studies, are difficult because of small cross sections involved. Direct beta-decay spectroscopy measurements are difficult due to the nature of electron/positron spectra. However, the beta-delayed radiation results in discrete spectra, which can be used to deduce detailed information of nuclear structure.

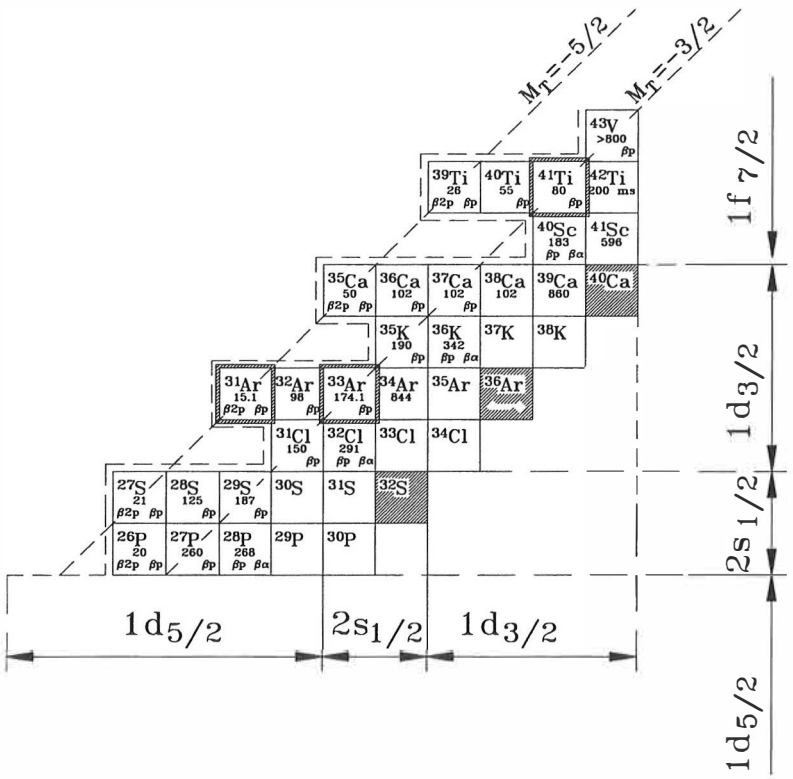

Figure 1. *Nuclide chart of proton rich-nuclei at the upper sd- and f- shells. The half-lives of nuclides ($t_{½}$<1s) are given in milliseconds and the particle emission modes are indicated. Shell model orbitals for proton and neutron occupation are shown. The nuclides studied in this work are indicated with hatched frames. The proton dripline is illustrated using the dashed line.*

The nuclide chart shown in **Figure 1** is illustrating nuclides in the area relevant to this work. In this work new results of the beta decays of two exotic nuclei, ^{41}Ti and ^{31}Ar, are presented. These nuclei lie in the region of sd- and fp-shells, where the standard shell model can be used as a reference. The M_T=-3/2 nucleus, ^{41}Ti is a special case due to its location across the Z=N=20 closed shells. The M_T= -5/2 nucleus, ^{31}Ar provides the most detailed data of the beta decay of an extremely proton-rich nucleus with a very large Q_{EC}-value.

2.1 Standard shell model

The concept of a shell model requires attractive potential. It is a fundamental assumption of the nuclear shell model that the central potential is collectively created by all of the nucleons. As fermions the nucleons are ruled by the exclusion principle. Therefore, they cannot occupy the same quantum state. This allows an assumption of individual orbits.

Nuclear magic numbers showed up experimentally as early as in the 1930's. They are an indication of a nuclear shell structure similar to an electron shell structure in atoms. However, explaining the shell closures by central potential only was not possible. Finally in 1949 the ***l*·*s***-coupling was introduced to explain the shell closures [16].

In shell model calculations the wave functions and energies of quantum states are obtained by solving the Schrödinger equation $H\Phi=E\Phi$ using an effective Hamiltonian. Operator H, consisting of a kinetic and two-body interaction terms, is taken as a sum of $H^{(0)}$ and $H^{(1)}$. The $H^{(0)}$ term consists of kinetic term T and a single particle potential U. The $H^{(1)}$ part is the so-called residual interaction and consists of two-body interactions W minus the single particle potential U [17]. To complete the calculation the residual interaction should be minimized. The procedure where residual interaction is minimized is called Hartree-Fock method [18]. In practice, the residual part of the Hamiltonian $H^{(1)}$ is minimized by choosing suitable potential.

The single particle energies and two-body interactions corresponding to $H^{(0)}$ and $H^{(1)}$, respectively are obtained, for example, from experimental binding energy differences. For shell model calculations in the sd- and fp-shells, good experimental effective interaction, such as USD (universal sd-shell interaction) [19] is available. The active orbitals are chosen so that the model

base for the calculation remains reasonable size. In this work calculations for the studied argon isotopes employed orbitals $1d_{5/2}$, $2s_{3/2}$, $1d_{3/2}$. For the beta decay of ^{41}Ti the model space was expanded to cover also $1f_{7/2}$, $2p_{3/2}$, $1f_{5/2}$ and $2p_{1/2}$ orbitals.

The standard calculations for beta decay strength are made using isospin formalism, where isospin is taken as a good quantum number. Thus, the single particle states are the same for both the protons and the neutrons. The diagonalization of the Hamiltonian matrix equations is done separately for different J,T combinations. However, the calculation including isospin mixing has to be done using pn-formalism, which expands the calculations. In the calculation of isospin mixing in the beta decay of ^{41}Ti the model space was reduced to consist of $1d_{3/2}$ and $1f_{7/2}$ orbitals only. More details of calculations involved in this work are presented in the relevant publications [Publ.2,3,4].

2.2 β-decay transition probabilities

In this work allowed beta decays were studied. Both the Fermi and Gamow-Teller decays are energetically possible in proton rich nuclei with $M_T<0$. In the Fermi decay the emitted positron (electron) has its spin opposite to the spin of the neutrino (antineutrino) and the spins couple to $S=0$ state. In the Gamow-Teller decay the spins are parallel and couple to $S=1$ state. Because the masses of the electron and the neutrino are small, their probability to transfer angular momentum is small. Therefore, the most probable transitions are $L=0$ with $\Delta J=0$ (Fermi) or $\Delta J=0,1$ (Gamow-Teller). The parity of the nuclear state is $\pi=(-1)^L$. Thus, for allowed transitions one obtains $\pi_i=\pi_f$.

2.2.1 Fermi matrix element

Squared matrix element for the Fermi beta-decay is [20]:

$$\langle M_F \rangle^2 = \langle J_f M T_f M_{Tf} | 1 \sum_{k=1}^{A} t_{\pm}(k) | J_i M T_i M_{Ti} \rangle^2 \qquad \textbf{(2)}$$

where J's are the total spins, M's are magnetic quantum numbers, T's are isospin quantum numbers, M_T's are isospin projections of initial and final states and $t_\pm$ is an isospin rising/lowering operator. Selection rules for the Fermi-beta decay can be concluded from the transition operators of the previous definition. The operator for the Fermi decay is $1\sum_k t_\pm(k) = 1T_\pm$. The part influencing on coordinate space is the unit operator, which does not change the spin. In addition, as a scalar it does not change the sign under parity operation, thus, it conserves the parity. The Fermi transition affects only on the orientation of isospin, i.e. $\Delta M_T=1$.

By the normalization of the wave functions the squared Fermi matrix element can be rewritten in a model independent form [20]:

$$\langle M_F\rangle^2 = T(T+1) - M_{Ti}M_{Tf} \qquad (3)$$

2.2.2 Gamow-Teller matrix element

Squared matrix element for the Gamow-Teller beta-decay is defined as [20]:

$$\langle M_{GT\pm}\rangle^2 = \frac{1}{2J_i+1}\sum_{mM_iM_f} |\langle J_fM_fT_fM_{Tf}|\sum_{k=1}^{A}\sigma_m(k)t_\pm(k)|J_iM_iT_iM_{Ti}\rangle|^2 \qquad (4)$$

To conclude the selection rules for allowed Gamow-Teller decay one needs to rewrite the previous definition in spherical coordinates [Publ.3]:

$$\langle M_{GT\pm}\rangle^2 = \frac{1}{2(2J_i+1)}\begin{pmatrix} T_f & 1 & T_i \\ -M_{Tf} & \pm 1 & M_{Ti}\end{pmatrix}^2 (\alpha_f J_f T_f \|\sum_{k=1}^{A}\sigma(k)\tau(k)\|\alpha_i J_i T_i)^2 \ , \qquad (5)$$

where the triple barred quantity is the transition matrix element reduced both in mechanical and isospace, α distinquishes states of the same JT and σ is the spin operator. The selection rules for the isospin are obtained from the 3j-symbol as follows: ΔT=0,1 and ΔM_T=1. The mechanical space part of the previous operator is the spin operator that does not change sign under parity operation.

2.2.3 Sum rule for the Gamow Teller decay

To be able to express the rates of allowed Gamow-Teller beta decays one would need exact information of all possible final and initial state wave functions. However, a model independent sum rule of the allowed Gamow-Teller transitions is given by [21]:

$$\sum_f (\langle M_{GT-}\rangle^2 - \langle M_{GT+}\rangle^2) = 3(N-Z) \qquad \textbf{(6)}$$

where the sum runs over all the final states. This gives a lower limit for the strength of the β^+ decay to be $\sum_f \langle M_{GT+}\rangle^2 > 3(Z-N)$, that is 9 for M_T=-3/2 and 15 for M_T=-5/2 nuclei.

2.3 Comparative half-life and transition probabilities

The partial decay rate of a transition is

$$\lambda_i = \frac{\ln(2)}{t_i}, \qquad \textbf{(7)}$$

where the partial half-life $t_i = t_{½}/b$, $t_{½}$ is the total half-life and b is the branching ratio for the transition in question. On the other hand the total beta-decay rate depends on the number of accessible final states, on the Coulomb field of a nucleus and on the product of the initial and the final state nuclear matrix elements. Integration over all the accessible states gives the quantity f_n known as the statistical rate function for n'th forbidden decay.

The product of the partial half-life t and the statistical rate function f is connected to the matrix elements as follows:

$$ft(1+\delta_R) = \frac{C}{\langle M_F\rangle^2(1-\delta_C) + \frac{g_A^2}{g_V^2}\langle M_{GT}\rangle^2} \quad \textbf{(8)}$$

where g_A is an axial vector coupling constant for a free neutron, $(1+\delta_R)$ is radiative and $(1-\delta_C)$ mixing correction. Constant C consists of several natural constants and of a vector coupling constant g_V. The values of δ_C and δ_R are typically smaller than 1%. The value of the vector coupling constant g_V is experimentally derived from the super allowed ($0^+ \rightarrow 0^+$) beta decays (where Gamow-Teller contribution is zero) and presently C equals 6145(4) s [22]. The ratio of the coupling constants can be obtained, for example, by using the experimental ft value of a free neutron and the squared matrix elements $\langle M_F\rangle^2=1$ and $\langle M_{GT}\rangle^2=3$ in **Equation (8)**. The value obtained in this way and used in the later analysis is $|g_A/g_V|=1.266$ [23].

In the studies of this thesis the f-values were obtained by interpolation from the tables of refs. [24]. The procedure used for calculating the experimental matrix elements introduces small uncertainty essentially larger than $(1+\delta_R)$ and $(1-\delta_C)$ to the f-values. Therefore, the theoretical corrections $(1+\delta_R)$ and $(1-\delta_C)$ were not used.

In the enclosed publications [Publ.3,4] and in this text the squared Fermi matrix element is abbreviated as $\langle M_F\rangle^2 = B(\mathrm{F})$. The squared GT matrix element multiplied by the ratio of coupling constant is abbreviated as $(g_A/g_V)^2\langle M_{GT}\rangle^2 = B(\mathrm{GT})$.

2.4 Particle emission from excited states

Excited states populated by the beta-decay are de-excited either by electromagnetic radiation or by emission of nuclear particles. Partial life-times for gamma-ray emission are typically longer than femto seconds. Due to the nature of the strong interaction the particle emission is a faster process.

However, the gamma-ray emission may compete with the particle emission when Coulomb and angular-momentum barriers delay particle emission. Competition between the particle and the γ-ray emission may be discussed in terms of ratios of partial widths:

$$\frac{\Gamma_\gamma}{\Gamma} = \frac{\Gamma_\gamma}{\Gamma_{p1}+\Gamma_{p2}+\ldots+\Gamma_\gamma} \qquad (9)$$

where Γ_γ is the gamma-decay width and Γ is the total width of the level in question. For proton-rich nuclei Γ_{pi}'s are most commonly the widths for p, α and 2p decays to ground and excited states.

In light nuclei, the upper limits of gamma-decay widths can be estimated by using the single particle limit according to ref. [25]. Otherwise, with a few exceptions, γ-decay widths are small for the levels above the proton separation energy S_p (**Figure 2**). For this reason, when approaching the proton dripline, exotic decay modes such as beta-delayed particle emissions are expected to dominate. The beta-delayed proton branch is proportional to the fifth power of a relative emission window ($1-S_p/Q_{EC}$) due to the beta decay phase space. Thus, nuclei with the smallest isospin projections M_T are strong β-delayed proton emitters (**Figures 2** and **3.**).

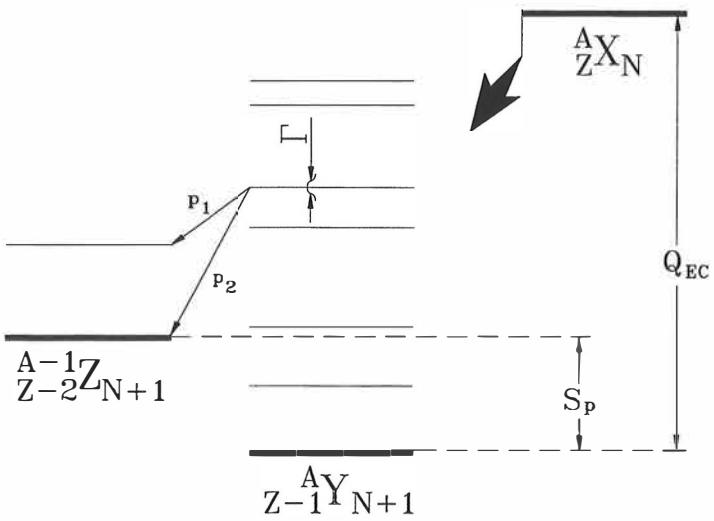

Figure 2. *Schematic figure of beta delayed proton emission to different final states.*

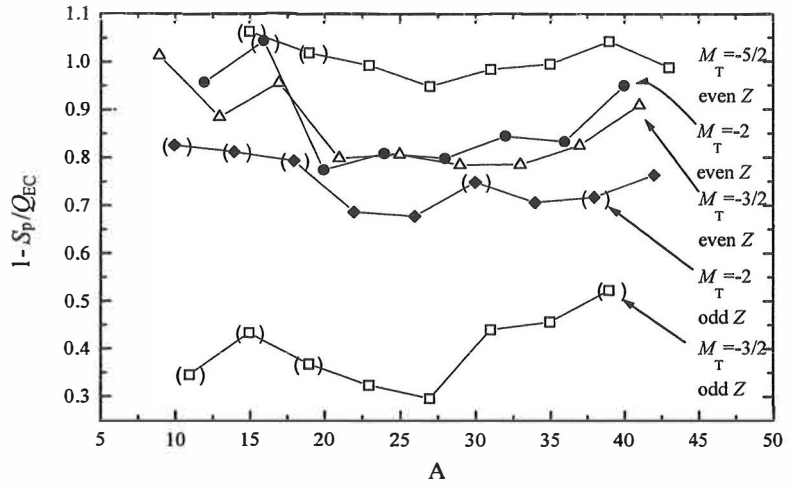

Figure 3. *The fraction of the proton emission window of the total beta decay window for proton precursors at p- and sd-shells. The dots in brackets show the unbound nuclei.[1]*

2.4.1 Proton emission

According to Heisenberg's uncertainty principle the life-time of the level is inversely proportional to its width. Thus, the partial width Γ_i is directly proportional to the partial decay constant λ_i. On the other hand, the partial width for a particle emission from a certain level is dependent on the barrier penetrability and spectroscopic amplitude, and can be expressed as [26]:

$$\Gamma_p = 2P_l\gamma_p^2 , \qquad \textbf{(10)}$$

where P_l is the barrier penetrability factor and γ_p^2 is the reduced particle decay width. The spectroscopic amplitude θ_p^2 is the transition probability between the initial and the final states and is included in the proton reduced width γ_p^2 as

$$\gamma_p^2 = \gamma_W^2 \theta_p^2 \qquad (11)$$

where γ_w^2 is the Wigner single-particle width.

For protons the barrier depends on both Coulomb and centrifugal forces. The angular momentum barrier V_l is dependent on the difference between the initial and final state spins, J_i and J_f. The angular momentum l carried away by the proton is limited by condition:

$$|J_i - J_f| - s_p \leq l \leq |J_i + J_f| + s_p \ . \qquad (12)$$

where $s_p = ½$ is the spin of the proton. The strong nuclear force conserves the parity symmetry $\hat{P}$. Therefore, in the particle emission the parity of a final state is given as $\pi_f = \pi_i(-1)^l$.

The barrier penetrability factor P_{lpi} is calculated using the regular (F_l) and irregular (G_l) Coulomb wave functions and the lowest l-value as described in ref. and is given as [8]:

$$P_l = \frac{kR}{F_l^2(R) + G_l^2(R)} \qquad (13)$$

where $k = (2\mu E)^{½}/\hbar$, μ is the reduced mass, E centre of mass energy for proton emission and R the nuclear radius. The Coulomb wave functions are obtained by solving the radial Schrödinger equation using Coulomb potential [27].

In cases, where more than one final state is involved, the particle decay widths can be compared directly to the ratio of spectroscopic amplitudes using the formula:

$$\frac{\Gamma_{p1}/P_{lp1}}{\Gamma_{p2}/P_{lp2}} = \frac{\theta_{p1}^2}{\theta_{p2}^2} \qquad (14)$$

where $\Gamma_{p1}/\Gamma_{p2} = I_{p1}/I_{p2}$ and I is the observed intensity (see [Publ.2]). In this case the protons p_1 and p_2 are emitted from the same initial state (**Figure 2**).

2.4.2 Isospin-forbidden particle emission

Proton emission from the isobaric analog states (IAS) with $T \geq 3/2$ to the final state is normally forbidden by the isospin selection rules. Nevertheless, such an emission is observed. The forbiddenness of the decay shows up as a narrow decay width. The components of wave functions with different T can explain the observed emission and suggest that the isospin is not a perfectly good quantum number. In the case of two mixed states with the same J^{π}, the wave function of the IAS can be expressed as:

$$|IAS\rangle = a|T\rangle + b|T'\rangle \qquad \textbf{(15)}$$

where a and b are the amplitudes of the corresponding unperturbed states of good isospin T and T', such that $T \neq T'$, and $a^2+b^2=1$.

In perturbation theory, mixing of two states with different T is described by the product of the mixing amplitudes:

$$ab = \frac{\langle T|H_{INC}|T'\rangle}{\Delta E} \qquad \textbf{(16)}$$

where ΔE is the energy difference of the perturbed states and H_{INC} is the isospin nonconserving Hamiltonian. Energy difference ΔE is important. At high excitation energies, near the IAS, there are often potential candidates for mixing. For the mixing in the final state of the proton decay, prominent levels are located at several MeV's apart. For sizeable mixing of $ab>0.01$ this would lead to unreasonably large isospin non-conserving matrix element $\langle T|H_{\mathrm{INC}}|T'\rangle$. Therefore, the mixing in the final state wave functions is expected to be small and the mixing in the proton emitting initial states need to be considered.

In beta-decay studies mixing can be determined, in principle, by comparing the observed Fermi strength to its model independent value given by **Equation (3)**.

$$B(F)_{th}\, a^2 = B(F)_{\mathrm{exp}} \qquad \textbf{(17)}$$

In this work the isospin mixing ($1-a^2$) was determined for the decay of ^{41}Ti [Publ.3]. In Chapter 4, an overview of the isospin mixing in proton-rich nuclei in the sd-shell is given.

2.4.3 Two-proton emission

Two-proton emission can be considered to happen either from the nuclear ground state or from excited states fed in beta decay. The ground state emission was predicted as early as 1961 by Goldansky [6], but it has not been observed experimentally. The first observation of two-proton emission as a beta-delayed process was made by Cable et al.[28]. Several mechanisms have been proposed: sequential, correlated and uncorrelated simultaneous emissions.

In some cases of potential ground state emitters, the sequential emission would be prohibited by the binding of a single proton. Thus, the only possibility would be simultaneous emission either as correlated (often called as ^{2}He) or uncorrelated emission of two protons. The correlated emission of two protons forming a S_0 state would be favoured by the non-existing angular momentum barrier.

In the sd-shell several nuclides with M_T=-2 or-5/2 have large enough excitation energy for the isobaric analogue states in their beta-decay daughter that the energy window for beta-delayed two-proton emission is wide enough. Despite strong phase space effect in the beta decay, the transition to the IAS is favoured. This is a consequence of the overlap in the wave functions of initial and final states. Thus the partial decay rate of a single 2p-emission channel becomes reasonably large.

In the case of the sequential emission from the T=5/2 state in the M_T=-3/2 daughter, the first proton decay could be favoured by the isospin allowed transition to the high lying intermediate state with T=2 or 3 admixture. In sequential emission the two protons would exhibit angular correlation analogous to gamma-ray cascades [29]. However, the correlations are expected to be weakened because the atomic electrons are breaking down the conservation of projection of nuclear angular momentum [30].

Two-proton decay from the T=5/2 state in ^{31}Cl competes with single proton emission. In addition to the effects of isospin, the barrier penetration factor contributes. Single proton decay to the ground state is possible only as an l=2 wave (assuming 5/2+ for the IAS). For the 2p-emission

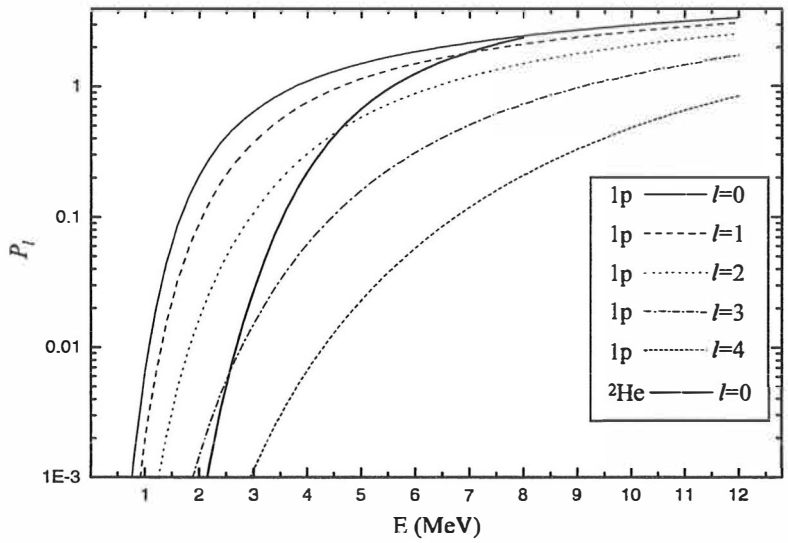

Figure 4. *Penetrability factors P_l for proton and ^{2}He emissions in ^{31}Cl.*

the decay Q-value is smaller, 7.6 MeV at maximum, but as seen in **Figure 4.** the penetrability factors for the ^{2}He emission with l=0 competes favourably with l=2 single proton emission to ground state of ^{30}S.

2.5 Isospin multiplets

Charge independency of the nuclear force leads to similarity of proton and neutron. The Coulomb force between the protons has to be considered as a charge symmetry breaking force. The states in the same isobar with the same isospin T are called isobaric analogue states and they form an isospin multiplet. The multiplet of T is formed by $2T$+1 states. In the vast majority of nuclides the nuclear ground state has isospin T=M_T, where M_T=1/2(N-Z). Thus, both "ends" of the isospin multiplet chain have the IAS as the nuclear ground state with T=M_T.

2.5.1 Isobaric multiplet mass equation

Applying the first order perturbation theory with charge symmetry breaking Hamiltonian to the energy of IAS's the parabolic dependence is obtained [31]. The quadratic form of an equation for IAS energies of the isospin multiplet was introduced by Wigner [32] and is given as:

$$E(\alpha T,M_T) = a(\alpha,T) + b(\alpha,T)M_T + c(\alpha,T)M_T^2 \qquad \textbf{(18)}$$

where parameters a, b and c are independent of M_T. This equation is generally called Isobaric Multiplet Mass Equation, IMME. **Figure 5** shows the isospin quadruplet [33] for the lowest T=3/2 states with A=41. Generally, IMME provides important means to derive exact masses for the proton-rich nuclei, provided that at least three members of the multiplet are known.

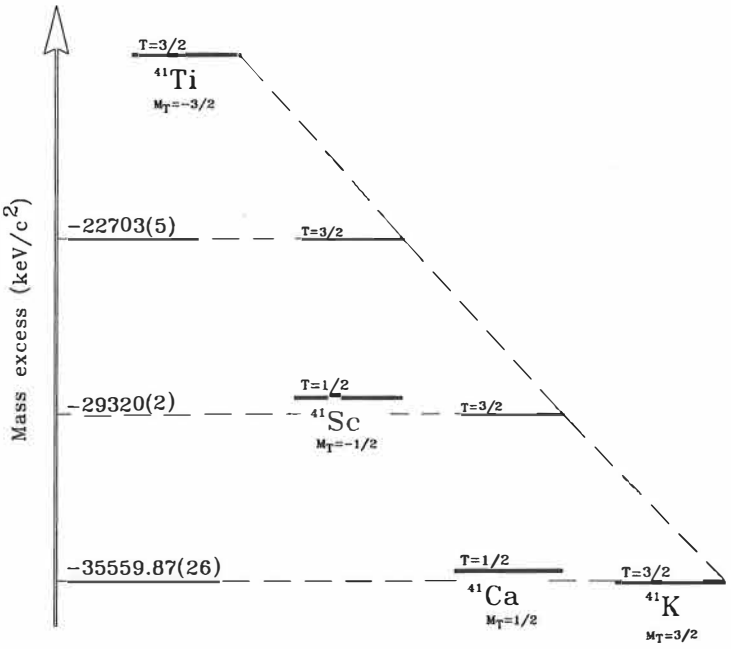

Figure 5. *T=3/2 isomultiplet of A=41. Mass excesses and level energies are taken from refs [1] and [33].*

Higher order corrections give rise to higher order terms in the IMME. However, T=3/2 isomultiplet in mass A=9 provides the only reliable evidence of deviation from the quadratic form [31]. A parameter d is used as constant of a cubic term in the IMME. Value of d is fitted in isospin quadruplet A=9 to be d = 5.8±1.5 keV [31]. Among the completely measured isospin quadruplets the overall values of d are generally consistent with zero. Therefore, in applications where Q_{EC} values are deduced the error rising from higher degree interactions can be neglected. In the isospin quintets for A=40 a deviation is also noticed [29]. However, it is probably due to large systematic uncertainty in the measured mass of ^{40}Ti.

Basically the analogue states of an isospin multiplet have similar wave functions. However, as pointed out the proton emission from the IAS to the ground state is isospin forbidden and takes place only through an impurity admixture in the initial state or final state wave function. The goodness of the isospin quantum number thus can be depicted by the emission of protons from the lowest isobaric analogue state. The appearance of isospin mixing in the IAS is considered to explain the deviations from the quadratic form.

2.5.2 Coulomb displacement energies

In cases where the isomultiplet is not completed so that a quadratic fit to energy levels of the same T is possible, the mass of the proton precursor can be deduced by using Coulomb displacement energy between the isobaric analog states (abbreviated as CDE), which is defined as [34]:

$$E_{CDE} - \Delta_{nH} = M(T, M_T) - M(T, M_T+1) \quad , \qquad \textbf{(19)}$$

where Δ_{nH} is the mass difference of a hydrogen atom and a neutron and M are masses of neighbouring isobaric analog states. Thus the Q_{EC} -value is the sum of the measured excitation energy of the IAS and E_{CDE}-Δ_{nH}. The values of E_{CDE} are obtained by fitting measured E_{CDE}'s as a function of $Z/A^{1/3}$. For example, the fit [34] to the measured E_{CDE} values of T=3/2 levels yielded a dependence E_{CDE} = 1411.1(3)$Z/A^{1/3}$-886.8(13) [keV]. These parameters together with the known E_{IAS} in ^{41}Sc give Q_{EC} = 13.068 MeV for ^{41}Ti, whereas the IMME provides Q_{EC} = 12.93(4) MeV.

The statistical errors of the parameters of E_{CDE} are small. However, the individual differences between the analog pairs are larger than tens of keV's. Therefore small statistical errors leading to small errors in Q_{EC} values are misleading and the result of the IMME is preferable.

3. Experimental methods

Short-lived isotopes studied in this work were produced in fusion evaporation reactions in ^{nat}Ca target by a ^{3}He beam and in spallation reactions in CaO target by a high-energy proton beam. Both of the elements studied in this work were mass separated using the on-line mass separators ISOLDE and IGISOL. Beta-delayed radiation from mass-separated sources was measured using a specially designed gas-silicon telescope and silicon, germanium and plastic scintillator detectors.

On-line isotope separation is a rather well established technique [35]. Several types of target-ion source concepts have been created to transport and ionize the reaction products. The two concepts used in this work are explained in the following two chapters.

3.1 ISOLDE

In the ISOLDE separator at CERN the nuclear reactions (spallation, fission and target fragmentation) are induced by 1 GeV proton beam [36]. The pulsed primary beam is produced by four parallel coupled proton synchrotrons. This combination is called PS-Booster [37]. A super cycle of 14.4 s consisting of 12 proton pulses with a 2.4 μs width is used at CERN. The intensity of each pulse can be varied from 1 to 3 x 10^{13} protons/pulse. Typically a maximum of seven pulses out of every super cycle are available at ISOLDE.

Reaction products are thermalised inside thick target material. The target is kept at high temperature to speed up diffusion of radioactive isotopes out of the target to the ion source. Ionization of atoms is done using different type of ion sources, such as plasma-, laser- and surface ion-sources. In principle, all different elements are possible to transport out of the target into the ion source. However, a long delay time associated with the release of refractory elements makes it difficult to apply this technique to all elements. Typical separation times for nonvolatile elements are from seconds up to tens of seconds. [38].

Due to diffusion, surface desorption and effusion inside the target and in the transfer line to the ion source, separator beam has a certain time structure. The release of a given element from the target follows the three-component exponential release function [39]:

$$P(t) = \frac{1}{Norm}(1-e^{-\lambda_r t})\,[\alpha e^{-\lambda_f t} + (1-\alpha)\,e^{-\lambda_s t}]\,, \qquad \textbf{(20)}$$

where subscripts r, f and s correspond to time-constant-like parameters of fast rise and fast and slow decay, respectively, and α is a weighting parameter. The release curve $P_i(t,\lambda_i)$ measured for radioactive ions includes additional exponential term describing radioactive decay losses ie. $P_i(t,\lambda_i)=P(t)\exp(-\lambda_i t)$.

For the target used in the ISOL339-experiment [Publ.2,5] the release was measured using long-lived radioactive argon atoms. The parameters λ_r, λ_f, λ_s and α were attained by fitting to be 50 ms^{-1}, 290 ms^{-1}, 900 ms^{-1} and 0.92, respectively. A cycle TDC-spectrum of ^{31}Ar is shown in **Figure 6** together with the simulated release curve calculated using **Equation (20)** and normalized to a measured intensity of ^{31}Ar using a constant shift.

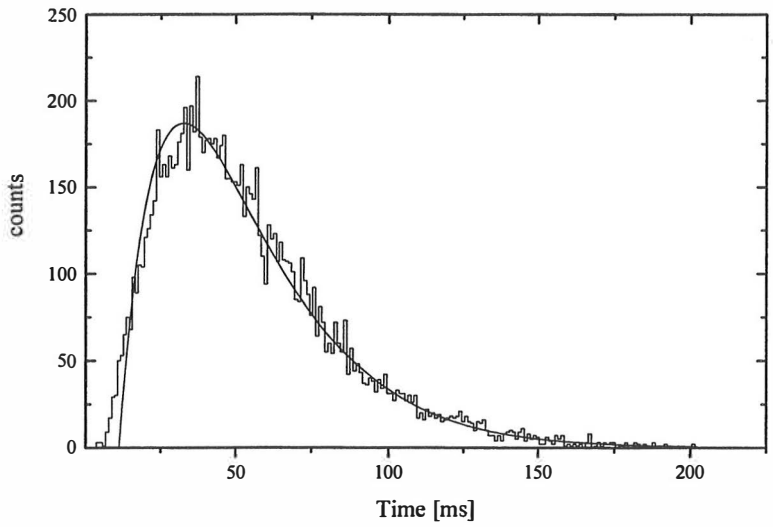

Figure 6. *Proton gated TDC spectrum of ^{31}Ar. The solid line is the release curve simulated using the equation given above and the fitted parameters given in the text.*

Argon isotopes were produced in spallation reactions in a 3.8 g/cm^2 thick CaO-powder target, which was kept at 1000° C temperature. The argon atoms diffusing out of the target were transported through a cooled transfer line to the ion source. This restricted transmission of other elements except noble gas atoms. Ionization was done using a plasma ion source.

In order to minimize the long-lived background activities at the measurement station the beam-on time or the beam gate of 150 ms was used. Production rates for ^{31}Ar and ^{33}Ar were ~2 and ~1000 atoms/s, respectively.

Mass resolving power of an isotope separator is defined as $R = M/\Delta M$, where ΔM is the full width at half maximum of a beam with mass M at the focal plane of the dipole magnet. To separate the neighbouring masses with the mass difference of about 1 atomic mass unit the resolving power of R>30 is needed for A=30 ions. The resolving power of the ISOLDE General Purpose Separator is typically 1000.

Most common contaminants in mass separated beams are chemical compounds of radioisotopes with stable oxygen and nitrogen isotopes. As an example, gamma-rays from ^{17}N were observed from A=31 radioactive source. A particle emitter produced in spallation reactions of calsium target and forming a A=31 or A=33 molecule with stable oxygen or nitrogen isotopes is ^{13}O transported in O_2 molecule with ^{18}O. However, a number of ^{13}O is reduced by the short half-life of ^{13}O ($t_{½}$=8.5 ms) and the small abundance of ^{18}O.

3.2 IGISOL

The IGISOL technique was developed in the middle of 1980's [40]. It is a novel ISOL method, in which contrary to traditional ISOL facilities, an ion source is not used. The reaction products recoiling out of a thin target are thermalised into helium. The helium pressure at the thermalization volume is on the order of 10 kPa.

Fusion-reaction products or fission fragments that recoil out of the target are energetic. They change their charge state continuously in collisions with target or buffer gas atoms. When ions finally reach low velocities ($V \lesssim 0.25 v_0$, where v_0 is the first Bohr orbital velocity [41]), their charge state is $0 \leq q \leq +2$. Due to impurities in the gas the +1 charge state is believed to dominate

at thermal velocities. The impurity molecules (H_2O, N_2, O_2 etc.) in the buffer gas have their ionization potentials in between the first and the second ionization potential of most of the elements. Therefore, the charge transfer from q=+2 to +1 can take place [40].

Reaction products are transported by the continuously flowing buffer gas through a nozzle and a skimmer into the high-vacuum section of the mass separator. Reaction products remain as q=+1 ions at least for an average evacuation time of the order of 1 ms. The evacuation time depends on the chamber geometry, on the flow conditions inside the target chamber and on diffusion, which is a function of the pressure [42].

Ions transported by super sonic helium flow are guided through a skimmer, which is at few hundred volts potential. After passing through the skimmer with a diameter of 1.3 mm, the ions enter the first stage of differential pumping where the residual gas pressure is brought down to 10^{-2} Pa. In this volume the pumping is done by a diffusion pump with a nominal capacity of 2000 ℓ/s.

In the upgraded IGISOL facility the pumping of the buffer gas is done by three 4200 m^3/h capacity roots pumps. An effective evacuation speed of the target chamber is more than 3000 m^3/h [43].

The ion beam passes through an extractor element to the high vacuum volume, where pumping is done by another diffusion pump with a nominal capacity of 1300 ℓ/s. The residual gas pressure in this volume is 10^{-4} Pa.

Acceleration of ions in the separator is done in two stages to avoid energy spread due to scattering in residual gas and to avoid high voltage sparking due to large potential difference over the modest vacuum volume. In the first differential pumping volume ions are accelerated using 10 kV potential. After the extractor electrode the q=+1 ions are accelerated to 38 keV total energy.

In the studies of ^{41}Ti a target of natural calcium manufactured by rolling to about 5 mg/cm^2 thickness was bombarded by a beam of 40 MeV ^{3}He ions. The ion beam of ^{3}He was provided by K=130 q^2/A [MeV] cyclotron. Beam intensities varied between 1 and 7 μA and a production rate of ^{41}Ti with the highest beam intensity was about 1 atom/second.

Mass resolving power, $R \approx 400$ was measured for the IGISOL separator in the experiment for ^{41}Ti. Therefore, a mass-separated beam yielded a clean source of A=41 reaction products. Selective

fusion evaporation reaction ^{40}Ca(^{3}He, xnyp) together with mass separation provides beams free of radioactive oxides. The isotope of ^{41}Ti is produced in 2n-channel.

3.3 Detector setups

Three different detector setups were used in the experiments to study the beta-decay properties of ^{31,33}Ar and ^{41}Ti nuclides (**Figure 7**). In all of the detector setups constructed for measurements of beta-delayed radiation the mass separated ion beams were implanted into thin carbon foils or a magnetic tape. The beta-delayed radiation was measured using combinations of gas-silicon, or silicon-silicon detector telescopes, scintillation detectors and germanium detectors. The gas-silicon telescope designed for the studies of this thesis is shortly discussed in the following chapter and in detail in [Publ.1].

3.3.1 Gas - silicon detector telescope

A gas-silicon detector telescope was designed to measure beta-delayed charged particles in the wide energy range. Beta-decay close to the proton drip-line is characterized by large Q_{EC}-values and large energy windows for delayed charged particle emission. Therefore, low-energy particle emission to excited states is probable. To measure beta-decay strength distribution in detail, a way to measure low-energy charged particles was developed.

Principle of novel identification method of emitted particles combined with high energy resolution was first presented in refs. [15], [44] and [45]. Commonly used silicon detector telescopes include thin ΔE detectors and thick E detectors. Due to a noise induced by large capacitance of thin ΔE detectors, the silicon telescopes suffer from deteriorated energy resolution.

To reduce the capacitance of a ΔE detector, a gas detector operated in proportional counter mode was chosen for the ΔE detector of the low-energy charged particle telescope. A thin gas layer is needed to allow protons with E≈200 keV to penetrate through the ΔE detector. Standard silicon detectors were chosen for an E detector.

Different detector gases were tested. Tetrafluoromethane (CF_4) was found to give the best amplification of the tested gases [Publ.1]. A gas pressure of about 10 mbar and a thickness of 6 mm results in effective thickness of about 25 $\mu g/cm^2$. A thin gas layer with a thin entrance window results in about 70 $\mu g/cm^2$ total thickness. For example, an extreme thinness of 8 μm of silicon corresponds to 1.8 mg/cm^2 and a range of a 600 keV proton.

Standard alpha particle sources were used to test the basic performance of the telescope. More detailed tests were done using a 2.5 MV van de Graaff accelelerator as a source of protons, deuterons and alpha particles. The wide energy loss distributions of test particles measured in the gas detector were explained by the Vavilov-theory [Publ.1].

The lower limits for measuring protons, deuterons and alpha particles were measured to be 155, 180 and 350 keV, respectively. The total energy resolution of about 20 keV for protons was determined using beta-delayed proton precursor sources.

A special method for the energy calibration of the gas telescope is needed to correct for nonlinearity of energy loss. Due to the smallness of the energy loss in the ΔE detector, the calibration is done only for the silicon detector. Calculated energy loss in the ΔE detector is subtracted from calibration energy. In contrary, true energies of the measured particles are obtained by adding calculated energy losses to measured energy. Energy loss values are interpolated from the tables of [46].

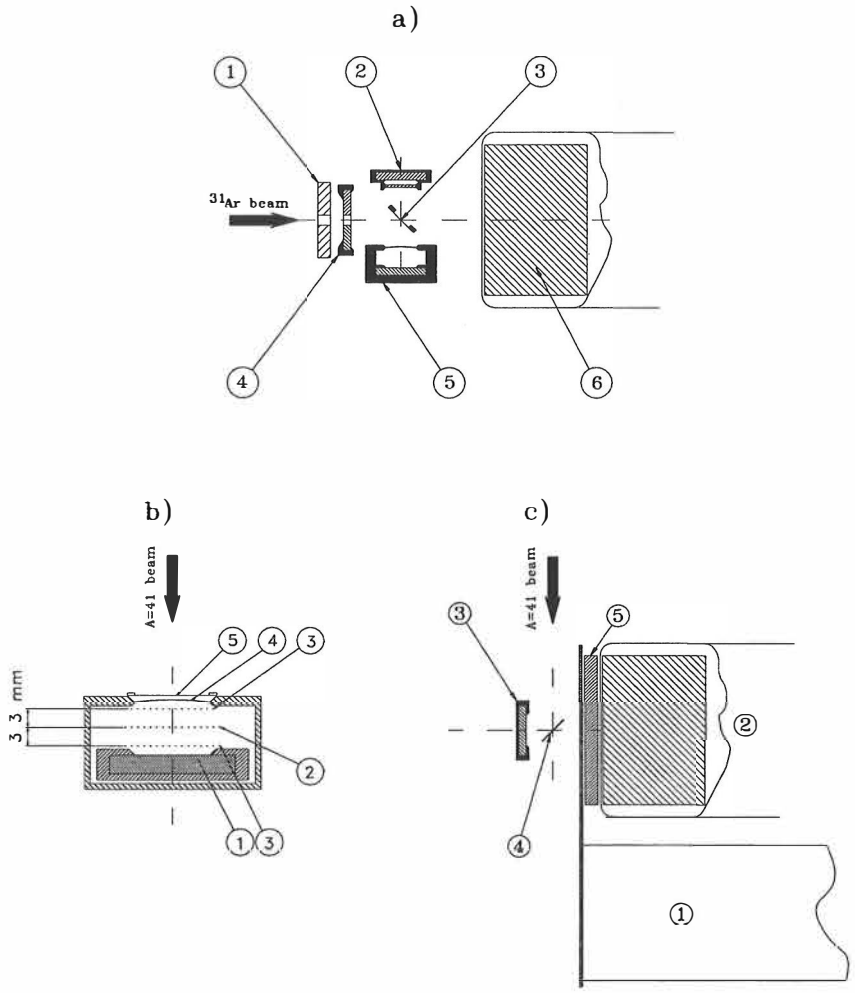

Figure 7. ***a)*** *The detector setup used in studies of ^{31}Ar and ^{33}Ar isotopes: collimator (1), silicon telescope (2), carbon foil (3), annular detector (4), gas telescope (5), germanium detector with 70% relative efficiency (6).* **b)** *The gas telescope used for measuring beta-delayed protons from ^{41}Ti: surface barrier detector (1), electrodes (anode 2, grounded grids 3), entrance window (4) and a 30 $\mu g/cm^2$ thick carbon foil (5).* **c)** *The detector setup used for measuring beta-delayed gamma-rays from ^{41}Ti: photo multiplier tube connected to a 0.9 mm thick plastic scintillator (1), germanium detector with 50% relative efficiency (2), ion implanted silicon detector (3), movable implantation tape (4) and 6 mm thick stainless steel absorber (5).*

4. Results and discussion

4.1 Particle emission from excited state

Beta-delayed proton and gamma-ray emissions were measured for all the nuclides studied in this work. Delayed two-proton emission was studied in the decay of ^{31}Ar. Significant competition between these modes was observed only in the decay of the IAS in ^{31}Cl, where decay branches of 2p and 1p emissions were measured. Proton emission branches from the same initial levels populating different final states were observed in all the studied nuclei. No gamma-rays from the beta-decay daughter were observed

In different reaction studies gamma-ray emission from levels of ^{41}Sc has been observed [33]. Several of those levels are populated by the beta-decay of ^{41}Ti. In this work the observed de-excitations of those levels were only due to 1p-emission. Beta decays to the lowest excited states are strongly favoured by the phase space. In addition, the effect of the Coulomb barrier hindering the proton emission is the strongest there. Therefore, the best possibility to observe competing gamma-rays are from the lowest proton unbound excited states. Based on the known sensitivity for gamma-ray observation [Publ.3], upper limit for Γ_γ/Γ -ratio can be set to $\lesssim 0.7$ for the levels at 2095.9 and 2666.6 keV. This agrees with the value measured earlier: $\Gamma_\gamma/\Gamma < 0.01$ [33]. For the decay of ^{31}Ar, the gamma-detection sensitivity was $\approx$1% and implies $\Gamma_\gamma/\Gamma < 0.04$ for the 2436 keV level, which is the most strongly populated one in the decay of ^{31}Ar.

4.1.1 Delayed proton emission

Proton spectra were measured with high energy resolution. The energies of the initial levels were deduced by using the measured energies of the transitions connecting them to the known final levels. Kinematic effects in the line shapes were taken into account for ^{33}Ar. The proton spectra

measured for all the studied nuclei using the gas telescope are presented in **Figures 8**, **9** and **10**. A typical feature in the beta-delayed proton spectra is summing of energies of proton and beta-particle. It is manifested for the most intensive transitions and is shown in all of the spectra in **Figures 8** , **9** and **10**.

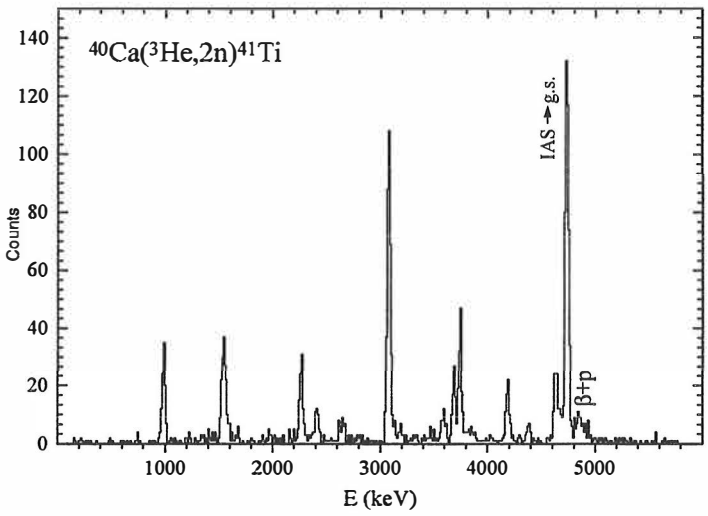

Figure 8. *The beta-delayed proton spectrum of ^{41}Ti measured using the gas telescope and the IGISOL mass separator [Publ.3].*

In total 25 and 36 different proton transitions were observed for the decay of ^{41}Ti and ^{31}Ar, respectively. All the observed transitions could be assigned to the decay of the nuclide of interest, because for the mass A=41 no other proton precursors were produced and for the masses A=33 and 31 the isotopic selection was done by using chemically selective ion-source - transfer-line combination. In the case of titanium all the transitions except two weak ones (E_i=5774 and 6468 keV) were assigned to decay to the ground state. The statistics in the spectrum above 5 MeV **(Figure 8)** was not high enough to extract the corresponding ground state transitions.

On the basis of measured delayed proton energies of ^{31}Ar, it was concluded that nine initial levels decay via more than one channel. Six different decay channels including three 2p-channels were assigned to the decay of the IAS in ^{31}Cl ([Publ.4], Table 2). Special attention was put on the analysis of the proton spectrum of ^{31}Ar, because individual protons of delayed 2p emission shows

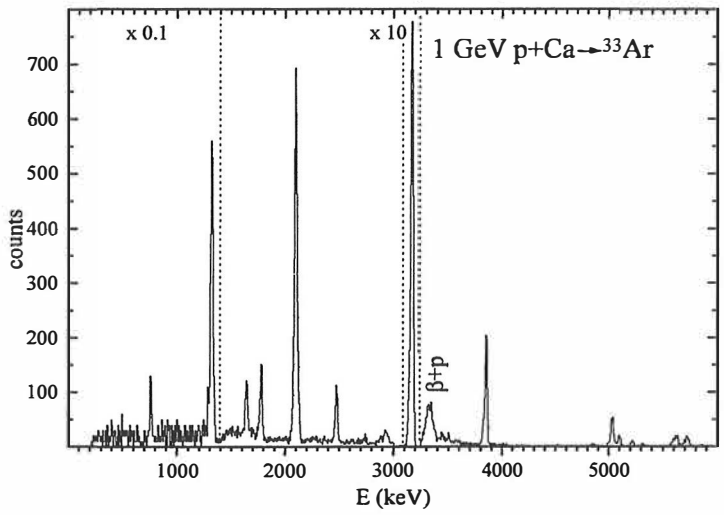

Figure 9. *Beta-delayed proton spectrum of ^{33}Ar measured using the gas telescope version described in [Publ.1]. Note the different scales for different energy regions.*

up continuous like background shown as dashed line in **Figure 10**. The background due to 2p -decay was deduced from the energy and intensity distribution of the individual protons of the 2p coincidences shown in **Figure 11**.

The emphasis for ^{33}Ar was put on the analysis of the transition pairs to different final states in order to study the spectroscopic amplitudes of proton emission. These transitions included one which was not observed earlier (768 keV). The analysis in [Publ.2] yielded six levels which decay by proton emission to two different final states. Two of these (5297 and 5870 keV levels) were potential candidates for isospin mixing. However, the spin-parity value of $J^{\pi}=3/2^{+}$ was suggested for them based on comparison of their decay patterns with that of the IAS ($J^{\pi}=1/2^{+}$) with the 100% branch to 0^{+} ground state.

Deduced ratios of spectroscopic amplitudes θ_{p1}/θ_{p2} (**Equation 14**) shows that the shell model predictions calculated with both the universal sd-shell interaction (USD)[19] and the Chung Wildenthal "Hole" (CWH)[47] interactions are in reasonable agreement with low energies. The measured energies are in good agreement with the shell model calculations, especially with the calculation using the CWH -interaction. The spectroscopic amplitudes provided by the shell model are well predicted by both of the used interactions.

The experimental results on ^{33}Ar together with their theoretical analysis show that a detailed and fruitful investigation of beta strength distribution of proton-rich nuclei is possible with a detector setup which allows delayed particle measurements with a high energy resolution and low energy threshold.

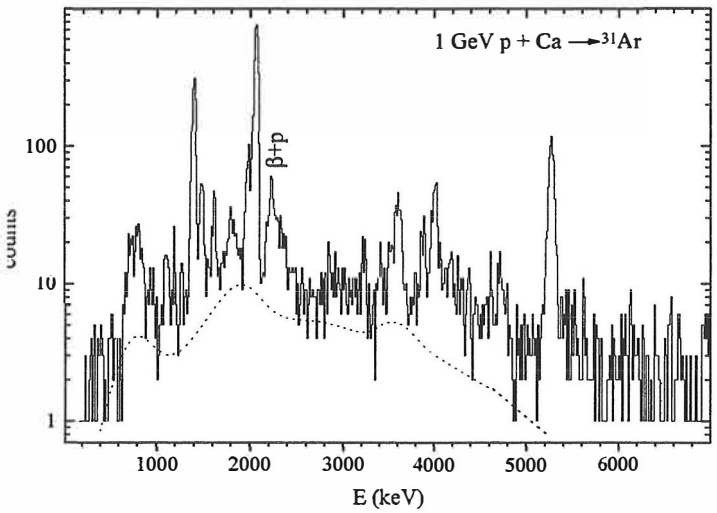

Figure 10 *The beta-delayed proton emission of ^{31}Ar. The dashed line shows the contribution of two-proton emissions.*

4.1.2 Two-proton emission

Decay mechanisms of the isobaric analog state of ^{31}Ar are discussed in [Publ.5]. **Figure 11** shows a two-proton coincidence matrix measured in the "180° geometry".

Three different 2p branches were assigned to the decay of the IAS. So far, the observed 2p-branches have been assigned to the decay of the IAS only. The present data concerning the beta-decay of ^{31}Ar implies for the first time a 2p-emission branch from other than isobaric analog state.

In the case of a sequential process, the intermediate nucleus ^{30}S has about 100 levels in the relevant energy region. Of course, all of these levels would not be involved. However, few levels involved with the decay could fade out the effect of angular correlations of sequential mode with the present statistics. If the mechanism is sequential and proceeds through several intermediate levels, the assumption of nearly continuous background in the single proton spectrum is still justified. Half of the protons from sequential decay will be observed as recoil broadened lines.

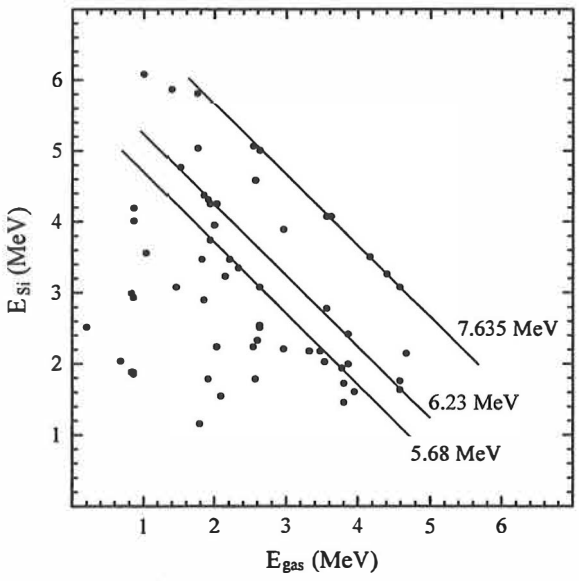

Figure 11. *Two-proton coincidences measured in 180° using the gas and the silicon telescopes. Assigned two-proton transitions from the IAS are indicated with lines and centre-of-mass energies.*

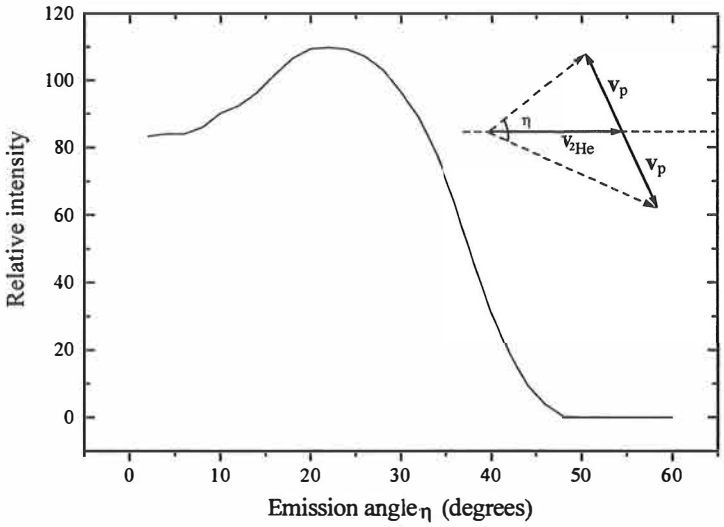

Figure 12. *Simulated angular distribution of ^{2}He emission observed in the laboratory frame as two separate protons. The simulation was done with $Q=E_{2He}+E_{BU}=7.635$ MeV and $E_{BU}\approx 0.6$ MeV at Gaussian distribution with FWHM=0.5 MeV. In the inset is shown the velocity vector presentation of the break up of ^{2}He in the centre-of-mass frame.*

In addition, as discussed in Chapter 2. the effect of angular correlations is not strong in the charged particle emissions. Finite solid angles needed for efficient detection also restrict accurate measurement of the angular correlations. Therefore, the energy spectra of individual protons with present statistics are not capable to expose the mechanism.

The emission of ^{2}He can be considered as a special case of simultaneous emission. In ref. [48] an approach of "semi-classical model" was employed to simulate measured angular distributions. In that simulation ^{2}He admixture was added on isotropic angular distribution. In [Publ.5] the same approach to solve the mechanism was used. A two-proton final state interaction E_{BU} was taken from the theoretical study of ref. [49]. In **Figure 12** a simulated angular distribution for a pure ^{2}He emission using an empirical final state interaction from ref. [50] is shown. In reality, the distribution of the break-up energy E_{BU} is skewed and exposes spread towards larger energies. However, the maximum of the angular distribution remains the same. The enhancement of the observed intensity at small angles ([Publ.5], Figure 5, upper panel) for the **7.6** MeV transition could, in principle, be a sign for a ^{2}He emission. On the other, the intensity distribution as a function of individual proton energy should be enhanced at energies of $E_p \approx Q_{2p}/2$. This is not observed in the data of ^{31}Ar.

As discussed in [Publ.5], the data can be interpreted by both the sequential and the simultaneous emission mechanisms. In the simultaneous noncorrelated emission mechanism the distribution of emitted protons depends on three-body phase space. The best fits were obtained for $5/2^+$ initial state. The results of the analysis were not capable to describe the data conclusively because of the lack of enough data points. In addition, the two-proton decay could in reality be characterized by a combination of different modes.

Based on the study in [Publ.5] a tentative assignment of $5/2^+$ for the IAS in ^{31}Cl was given. No final conclusion of the two-proton decay mechanism is provided.

4.2 Isospin mixing

4.2.1 T=3/2 state in ^{41}Sc

Isospin mixing in the lowest T=3/2 state in ^{41}Sc was studied in [Publ.3] and substantial mixing was observed. Based on the missing intensity, the amount of mixing was judged to be >4%. A value of 10(8) % was adopted using B(GT) from the shell model calculation and the deduced quenching in the beta decay of ^{41}Ti.

A subsequent shell model calculation in the pn-formalism using the $d_{3/2}$-$f_{7/2}$ model space with isospin breaking Hamiltonian gave the Fermi strength B(F)=2.76 for the IAS [51]. This leads to a theoretical mixing intensity $1\text{-}a^2 = 1\text{-}\ 2.76/3.00 = 8.0$ %. This value was obtained by assuming overlap integrals for single-particle radial wave function of the proton and the neutron to be equal to one. Thus, in reality, the mixing would be slightly larger. However, the theoretical value is in excellent agreement with the observation.

Based on the calculation the missing strength from the IAS of ^{41}Ti is mainly concentrated in the level located 41 keV below the IAS. Experimentally, we observe levels 55 and 99 keV below the IAS as potential candidates to generate the mixing.

4.2.1 Other states

In **Table 1** the isospin mixing values derived for the IAS's of some beta-delayed proton precursors are compiled. The isospin mixing has fundamental importance in determining the vector coupling constant g_V and its ratio to axial vector coupling constant g_A/g_V. The correction's δ_c (**Equation 8**), which mainly arise from nonperfect radial overlapping of initial and final state wave functions are also presented in **Table 1** and are obtained from ref. [52].

Table 1. *Isospin mixing in the lowest isobaric analog states in some beta-delayed proton precursors in the upper sd-shell and crossing of sd- and fp-shells. The shell model calculations are made with USD interaction.*

Nucleus	$\langle M_F \rangle^2$	Deduced mixing $1\text{-}a^2$ (%)	refs.	δ_c (%) [52]	Shell model $1\text{-}a^2$ (%) [53]
^{33}Ar	2.7(3)	9(9)	[8]	1.32	0.6
^{37}Ca	2.89[a]	$3.8^{+0.2}_{-0.8}$	[54]	0.52	0.4
^{41}Ti	2.69(22)	10(8)	[Publ.3]	0.56	8.1
^{32}Ar	4.1(5)	0^{+10}_{-0}	[55]		1.1
^{36}Ca	4.0(2)	0^{+3}_{-0}	[56]		0.4
^{40}Ti	3.94(26)	2^{+6}_{-2}	[57][b]		17.3
^{31}Ar	$3.2^{+3.0}_{-0.3}$	<40	[Publ.4]		7.4

All the matrix elements are calculated using the measured intensities, half-lives and excitation energies obtained from listed references, log f tables of Gove and Martin [24] and C − 6145(4) s. Because the experimental strength is a sum of the Fermi and the Gamow-Teller strengths, the "quenched" shell model value is subtracted except in case of ^{33}Ar, where upper limit of B(GT) is given in [10].

[a] Value obtained from the mixing amplitude a = 0.981 measured in [54].

[b] Another measurement [58] introduces more strength than predicted by the Fermi -matrix element

Based on the results of **Table 1** the isospin mixing in the wave function of the IAS is significant in the odd-A nuclei. In addition, it should not be neglected in the 0+→ 0+ decay studied, especially when decays above mass A=40 are examined.

The difficulty in predicting the mixing is obvious. When the energy difference between the predicted levels is large, the mixing of the levels is small (**Equation 16**). The shell model

calculations are not capable to predict the level energies precisely enough, at least when using the USD interaction.

For ^{31}Ar the intensity missing from the IAS is puzzling. Strong mixing is predicted in that case also. However, the mixing cannot explain the missing intensity as discussed in [Publ.4].

4.3 Beta decay strength

The measured total Gamow-Teller strengths for ^{41}Ti in the energy interval from 0 to 8 MeV and for ^{31}Ar from 0 to 14 MeV were 3.6(5) and 3.4(5), respectively. Shell model calculations yielded total strengths 5.6 for ^{41}Ti and 8.4 for ^{31}Ar in the corresponding energy windows, respectively. The reduction of the measured beta-decay strength in comparison with the calculated one is called quenching of the beta decay strength. The quenching factor is defined as $q=(\sum B(GT)_{exp}/\sum B(GT)_{theor})^{½}$ [59]. In ^{31}Ar the GT-quenching for the ground state and the first two excited states is already q=0.64. This is the same as the total quenching observed within the 14 MeV observation window. Below 5.5 MeV excitation in ^{31}Cl, the quenching q is about 0.71.

Quenching factors of some proton-rich isotopes in the upper sd-shell and at the crossing of sd- and fp-shells are compiled in **Table 2.** The shell model calculations with the USD interaction for argon and calcium isotopes are available in the literature as given in **Table 2.** As an exception, calculation with CWH interaction was available for ^{38}Ca. For titanium isotopes ^{40}Ti and ^{41}Ti, the Hamiltonian consisted of the USD interaction for the sd-shell, while two-body matrix elements for the crossing region between the shells were generated with the Millener-Kurath potential and for the fp-shell they are obtained from van Hees and Glaudemans [Publ.3][60]. The interaction used in calculation for ^{43}Ti is described in [61]. The quenching given below is determined inside the measurement window given in the references.

Among sd-shell nuclei the quenching factor of q=0.77 has been generally deduced [62]. Often the quenching is simplified to be the reduction in axial vector strength [63], i.e. the ratio between the axial vector coupling constant for a free neutron and an effective coupling constant: $g_A^*/g_A \approx 0.77$. This phenomenon is discussed as a renormalization of the weak axial vector current

in nuclei [64]. Raman et al. [52] have suggested the quenching arising from the presence of strong interactions in the nuclear medium, which renormalises the axial vector coupling constant.

Based on the results given in **Table 2** the quenching for the proton-rich nuclei at the upper sd-shell is smaller on average than the "standard" value. In addition, the quenching factor is approaching 1 within M_T=-3/2 and -2, argon and calcium isotopes, while for the titanium isotopes the quenching seems to be on the generally recognized level. The total experimental and theoretical strengths within the measurement window are presented in **Figure 13.**

The calculation predicts only 24 final levels for ^{41}Ti within the measurement window, whereas 33 levels were observed. The calculation of beta decay of ^{31}Ar showed the opposite behaviour. More than 200 levels were predicted while only 23 were observed. This is partly explained by the sensitivity limit of the measurement. In addition, the fragmented decay patterns of beta decay final states in ^{31}Cl together with finite energy resolution for proton detection could lead to the interpretation of a smaller number of final states than exist in reality. This a well-known effect (Pandemonium [65]), which can also influence the total quenching, however if weakly populated levels were observed at higher excitation, the quenching of the lower levels would remain (or be increased slightly). In summary, it is obvious from the present results that ^{31}Ar possesses anomalous behaviour in terms of quenching.

Table 2. *Beta-decay quenching factors of proton-rich argon, calcium and titanium isotopes.*

M_T	Ar	Ca	Ti
-1/2	0.81(5)	[a]	0.73(5)
-1	0.97[b]	0.747(14)	[a]
-3/2	1.09(19)	0.92(5)	0.80(10)
-2	0.86(9)	0.96(9)	0.64(6)[c]
-5/2	0.64(5)	[d]	[a]
mean	0.874	0.876	0.73

The quenching factors are deduced within the given beta decay measurement window from the references: [55], [63], [9], and [Publ.4] for argon isotopes; [66],[67] and [20] for calcium isotopes; [54], [60], [61] and [Publ.3] for titanium isotopes.

[a] The beta decay distribution is not known experimentally.

[b] The error limit is not available.

[c] Another measurement of beta decay of ^{40}Ti [57] yielded q=0.79(6).

[d] The beta decay of ^{35}Ca has recently been measured at Ganil. The quenching is roughly the same as in the other listed calcium isotopes [68].

Based on the present knowledge it is difficult to draw a conclusion whether the axial vector current would be renormalised from a free nucleon value. However, the quenching is needed to bring the theory and experimental results in agreement. On the other hand, the quenching is necessarily model dependent. This has been shown in ref. [63], where measured strengths within Ar-isotopes are compared with two shell model calculations done using the USD and the CWH interactions. This is rather obvious conclusion, because quenching is deduced based on the comparison between the $\sum B(\mathrm{GT})_{exp}$ and $\sum B(\mathrm{GT})_{theor.}$ values, which are proportional to the matrix elements. The calculated location of a Gamow-Teller resonance can vary for different interactions, and therefore, be the main source of quenching as discussed in [63]. In addition, the $\sum B(\mathrm{GT})_{exp}$ is always determined from the limited measurement window. Thus, the minor part of

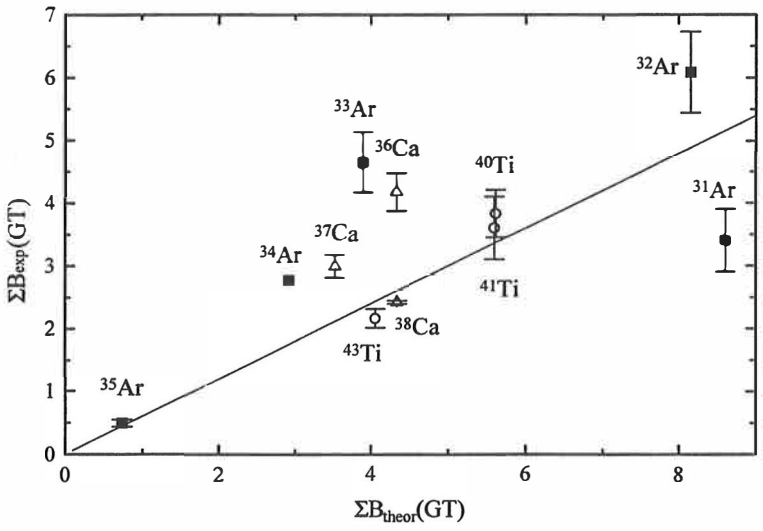

Figure 13 *The total experimental GT-strength vs. theoretical one for some proton-rich argon, calcium and titanium isotopes deduced from the measurement window. The line shows the "standard" quenching of q=0.77.*

the quenching can arise from the incompletely distributed intensity.

An explanation of beta-strength quenching is discussed in terms of the core polarization and subnucleonic degrees of freedom [69]. The shell-model introduces excess of strength to the levels predicted within the measurement window. This explanation is generally referred as core

polarization. The mesonic effects represented, for example, by delta resonances effect practically similar to the core polarization by taking a share of the strength. The first of the effects could, in principle, be restricted in "super" large scale calculations where the model space would be expanded. The latter is beyond the standard shell model approach.

5. Conclusions and outlook

In this work beta-decay properties of three different proton-rich nuclei were studied. All these nuclei are characterized by a strong beta-delayed proton branch. The beta decays of ^{41}Ti and ^{31}Ar were measured to populate levels that entirely de-excite by the emission of protons with some negligible upper limits for alpha particle and gamma-ray emission branches.

In the decay of ^{31}Ar the main feature was a very complex decay pattern. This complicated the interpretation of the beta-decay branchings. The beta-decay was observed to populate excited states as high as 14.5 MeV. Comparison with the shell model calculation done at the full sd-shell space using the USD interaction yielded a quenching factor of q=0.64(5) within the experimental energy window. In comparison with other recently measured beta-decay strengths for proton-rich nuclei, the measured quenching factor differs from the general trend.

Spectroscopic amplitudes were studied for the beta-delayed proton decay of ^{33}Ar. Quite good predictions are provided by both of the interactions used in the shell model calculation. This suggests that the level structures are predicted well.

Quenching for the beta decay of ^{41}Ti was deduced to be q=0.80(10), which agrees with the general trend observed for light proton-rich nuclei. The isospin mixing in the isobaric analog state was deduced from the measured beta-decay strength. The experimental value of mixing agrees with the shell-model value calculated in the reduced model space. However, a sample of mixing values for proton-rich nuclei implied that the shell model calculation cannot provide reliable values for further applications.

Three different two-proton branches were observed to de-excite the IAS in ^{31}Cl. Due to modest statistics combined with the limitations of the detector setup, energy and angular distributions were not able to expose the 2p-decay mechanism definitely.

New experimental techniques were developed for the detection of delayed radiation. However, to improve the quality of the proton spectra, higher granularity measurement setups are needed in future. For this reason a 2π detector array consisting of 15 gas-silicon detector telescopes has been developed[70]. This device provides a total geometrical efficiency of 18% for individual

particle detection. A probability of summing the proton and the preceding beta particle is only 1.2 %.

Main advantage of the high granularity array is in the study of 2p emission. The efficiency for two-particle detection is proportional to the number of detector pairs, which is greatly increased in comparison to the setup used in this work. The detector array has very recently been used in two experiments where the decay mechanism of two-proton emission from the levels of ^{31}Cl was studied. Based on the preliminary results, several sequential branches were found.

References

1. G. Audi and A.H. Wapstra, Nucl. Phys. **A 565** (1993) 1.

2. B.A. Brown, A. Etchegoyen and W.D.M. Rae, *The computer code OXBASH*, MSU-NSCL report 524 (1988).

   E. Caurier, *Shell Model code Antoine*, Strasbourg 1989, private communication.

3. C.W. Kim and A. Pevsner, *Neutrinos in physics and astrophysics* (Harwood academic publishers, Chur, Switzerland, 1993).

4. ICARUS Collaboration, *ICARUS II Proposal,* LNGS Repost 94/99-I (1993)

5. I. Mukha, M.J.G. Borge, D. Guillemaud-Mueller, P. Hornshøj, F. Humbert, B. Jonson, T.E. Leth, G. Martinez Pinedo, T. Nilsson, G. Nyman, K. Riisager, G. Schrieder, M.H. Smedberg, O. Tengblad, K. Wilhelmsen Rolander and the ISOLDE Collaboration, Phys. Lett. **B 367** (1996) 65.

6. V.I. Goldansky, Nucl. Phys. **27** (1961) 648.

7. J. Gorres, M. Wiesher,F.-K. Thielemann, Phys. Rev. **C 51** (1995) 392.

8. J.C. Hardy, J.E. Esterl, R.G. Sextro and J. Cerny, Phys. Rev. **C 3** (1971) 700.

9. M.J.G. Borge, P. Dessagne, G.T. Ewan, P.G. Hansen, A. Huck, B. Jonson, G. Klotz, A. Knipper, S. Mattsson, G. Nyman, C. Richard-Serre, K. Riisager, G. Walter and the ISOLDE collaboration, Phys. Scr. **36** (1987) 218.

10. D. Schardt and K. Riisager, Z.Phys. **A 345** (1993) 265.

11. V. Borrel, J.C. Jacmart, F. Pougheon, A. Richard, R. Anne, D. Bazin, H. Delagrange, C. Detraz, D. Guillemaud-Mueller, A.C. Mueller, E. Roeckl, M.G. Saint-Laurent, J.P. Dufour, F. Hubert and M.A. Pravikoff, Nucl. Phys. **A 473** (1987) 331.

    D. Bazin, R. Del Moral, J.P. Dufour,A. Fleury, F. Hubert, M.S. Pravikoff, R. Anne, P. Bricault, C. Detraz, M. Lewitowicz, Y. Zheng, D. Guillemaud-Mueller, J.C. Jacmart, A.C. Mueller, F. Pougheon and A. Richard, Phys. Rev. **C 45** (1992) 69.

    V. Borrel, J.C. Jacmart, F. Pougheon, R. Anne, C. Detraz, D. Guillemaud-Mueller, A.C. Mueller, D. Bazin, R. Del Moral, J.P. Dufour, F. Hubert, M.S. Pravikoff and E. Roeckl and Nucl. Phys. **A 531** (1991) 351.

12. M.J.G. Borge, H. Cabelmann, L. Johannsen, B. Jonson, G. Nyman, K. Riisager, O. Tengblad and ISOLDE collaboration, Nucl. Phys. **A 515** (1990) 21.

13. R.G. Sextro, R.A. Gough and J. Cerny, Nucl. Phys. **A 234** 130.

14. Z.Y. Zhou, E.C. Schloemer, M.D. Cable, M. Ahmed, J.E. Reiff and J. Cerny, Phys. Rev. **C 31** (1985) 1941.

15. D. M. Moltz, J.D. Robertson, J.C. Batchelder and J. Cerny, Nucl. Instr. and Meth. **A 349** (1994) 210.

16. O. Haxel, J.H.D. Jensen and H.E. Suess Phys. Rev. **75** (1949) 1766.

M.G. Mayer Phys. Rev. **75** (1949) 1969.

17. K.L.G. Heyde, *The Nuclear Shell Model*, Second Edition (Springer-Verlag, Berlin, 1994,).

18. S.S.M Wong, *Introductory Nuclear Physics* (Prentice Hall, New Jersey, 1990) p. 291.

19. B.A. Brown and B.H. Wildenthal, At. Data. Nucl. Data Tables **33** (1985) 347.

20. P.J. Brussaard and P.W.M Glaudemans, *Shell Model Applications in Nuclear Spectroscopy* (North-Holland, New York, 1977)

21. K. Ikeda, S. Fujii, J.I. Fujita, Phys. Lett. **2** (1962) 169.

I. Talmi, *Simple Models of Complex Nuclei* (Harwood, Chur, 1993) p. 130.

22. I. Towner, E. Hagberg, J.C. Hardy, V.T. Koslowsky and G. Savard, Int. Conf. on exotic nuclei and atomic masses , ENAM 95, Arles, 1995, eds. M. De Saint Simon and O. Sorlin (Editions Frontiers, Gif-Sur-Yvette, 1995) p.711.

23. K. Schreckenbach, P. Liaud, R. Kossakowski, H. Nastoll, A. Bussiere and J.P. Guillaud, Phys. Lett. **B 349** (1995) 427.

24. N.B. Gove and M.J. Martin, Nucl. Data Tables **10** (1971)

Ph. Dessagne and Ch. Miehe, Strasbourg, CRN report CRN PN 87-08

25. A. Bohr and B. Mottelsson, *Nuclear Structure* **Vol I** (W.A. Benjamin, New York, 1969).

26. B. A. Brown, Phys. Rev. Lett. **65** (1990) 2753.

A. M. Lane and R.G. Thomas, Rev. Mod. Phys. **30**, (1958) 257.

M.H. Macfarlane and J.B. Franch, Rev. Mod. Phys. **32** (1960) 567.

27. M.A. Preston, *Physics of The Nucleus* (Addison-Wesley publishing company inc., Massachusetts, 1962) p. 360.

28. M.D. Cable, J. Honkanen, R.F. Parry, S.H. Zhou, Z.Y. Zhou and J. Cerny, Phys. Rev. Lett. **50** (1983) 404.

J. Äystö, D. M. Moltz, X.J. Xu, J.E. Reiff and J. Cerny, Phys. Rev. Lett. **55** (1985) 1384.

29. J. Äystö and J. Cerny, in *Treatise on Heavy Ion Science*, **Vol 8** (Plenum Press, New York, ed. D.A. Bromley, 1989) p. 207.

30. J.O. Rasmussen, in *Alpha- Beta- and Gamma-ray spectroscopy* **Vol I** (North-Holland, Amsterdam, 1966, ed. K. Siegbahn) p. 703.

31. N. Auerbach, Phys. Rep. **98** No.5 (1983) 273.

32. E.P. Wigner, in Proc. of the Robert A. Welch Foundation Conference on Chemical Research, Houston, 1957 (ed. W.O. Millikan) p. 67, unpublished.

33. P.M. Endt, Nucl. Phys. **A 521** (1990) 1.

34. M.S. Antony, A. Pape and J. Britz, At. Data and Nucl. Data Tables **66** (1997) 1.

35. H.L. Ravn and B.W. Allardyce, in *Treatise on Heavy-Ion Science* **Vol 8**, (Plenum Press, New York, ed. D.A. Bromley, 1989) p. 363.

36. E. Kugler, D. Fiander, B. Jonson, H. Haas, A. Przewloka, H.L. Ravn, D. J. Simon, K. Zimmer and the ISOLDE collaboration, Nucl. Instr. and Meth. **B 70** (1992) 41.

37. ISOLDE PS Booster Facility at CERN: Experiments with slow radioactive beams, Nucl. Phys. News **Vol. 3**, No. 2 (1993)

38. R. Kirchner. Nucl Instr. and Meth. **186** (1981) 275.

P. Hoff, O.C. Jonsson, E. Kugler and H.L. Ravn, Nucl Instr. and Meth. **221** (1984) 313

39. J. Lettry, R. Catherall, P. Drumm, P. Van Duppen, A.H.M. Evensen, G.J. Focker, A. Jokinen, O.C. Jonsson, E. Kugler, H. Ravn and the ISOLDE collaboration, Nucl. Instr. and Meth. **B 126** (1997) 130.

40. J. Ärje, J. Äystö, H. Hyvönen, P. Taskinen, V. Koponen, J. Honkanen, K. Valli, A. Hautojärvi and K. Vierinen, Nucl. Instr. and Meth. **A 247** (1986) 431.

41. V.S. Nikolaev and I.S. Dmitriev, Phys. Lett. **28 A** (1968) 277.

42. K. Peräjärvi et al., Nucl. Instr. and Meth. A, To be published.

43. H. Penttilä, P. Dendooven, A. Honkanen, M. Huhta, P.P. Jauho, A. Jokinen, G. Lhersonneau, M. Oinonen, J.-M. Parmonen, K. Peräjärvi and J. Äystö, Nucl. Instr. and Meth. **B 126** (1997) 213.

44. J.D. Robertson, J.E. Reiff, T.F. Lang, D.M. Moltz and J. Cerny, Phys Rev. **C 42** (1990) 1992.

45. M.W. Rowe, D.M. Moltz, J.C. Batchelder, T.J. Ognibene, R.J. Tighe and J. Cerny, Nucl. Instr. and Meth. **A 397** (1997) 292

46. Stopping powers and ranges for protons and alpha particles, ICRU Report 49, International Comission on Radiation Units and Measurements, Bethesda, Maryland, USA, 1993.

47. W. Chung, Ph.D Thesis, Michigan State University, 1976.

B.H. Wildenthal and W. Chung in *Mesons in Nuclei* (North-Holland, eds. M. Rho and D.H. Wilkinson, 1979), p. 723.

48. R. Jahn, L.R. McGrath, D.M. Moltz, J.E. Reiff, X.J. Xu, J.Äystö, J. Cerny, Phys. Rev. **C 31** (1985) 1576.

49. R.J.N. Phillips, Nucl. Phys. **53** (1964) 650.

50. T.V. Congedo, I.S. Lee-Fan and B.L. Cohen, Phys Rev **C 22** (1980) 985.

51. P.O. Lipas, private communication.

52. S. Raman, C.A. Hauser, T.A. Walkiewicz and I. Towner, At. Data and Nucl. Data Tables **21** (1978) 567.

53. T.Siiskonen, private communication.

54. N.I. Kaloskamis, A. Carcia, S.E. Darden, E. Miller, W. Haeberli, P.A. Quin, B.P. Schwartz, E. Yacoub, E.G. Adelberger, Phys. Rev. **C 55** (1997) 640.

55. T. Bjørnstadt, M.J.G. Borge, P. Dessagne, R.-D. Dincklage, G.T. Ewan, P.G. Hansen, A. Huck, B. Jonson, G. Klotz, A. Knipper, P.O. Larsson, G. Nyman, H.L. Ravn, C. Richard-Serre, K. Riisager, D. Schardt, G. Walter, and The ISOLDE Collaboration, Nucl. Phys. **A 443** (1985) 283.

56. W. Trinder, E.G. Adelberger, B.A. Brown, Z. Janas, H. Keller, K. Krumbholz, V. Kunze, P. Magnus, F. Meissner, A. Piechaczek, M. Pfützner, E. Roeckl, K. Rykaczewski, W.-D. Schmidt-Ott, M. Weber, Phys. Lett. **B 348** (1995) 331.

57. W. Trinder, R. Anne, M. Lewitowicz, M.G. Saint-Laurent, C. Donzaud, D. Guillemaud- Mueller, S. Leenardt, A.C. Mueller, F. Pougheon, O. Sorlin, M. Battacharya, A. Garcia, N.I. Kaloskamis, E. G. Adelberger, H.E. Swanson, GANIL preprint P97 24.

58. W. Liu, M. Hellström, R. Collatz, Benlliure, L. Chulkov, D. Cortina Gil, F. Farget, H. Grawe, Z. Hu, N. Isawa, M. Pfützner, A. Piechaczek, R. Raabe, I. Reusen, E. Roeckl, G. Vancraeynest and A. Wöhr, Z.Phys. **A 359** (1997) 1.

59. G. Martinez-Pinedo, A. Poves, E. Caurier and A.P. Zuker, Phys. Rev. **C 53** (1996) R2602.

60. W.E. Ormand, P.M. Pizzochero, P.F. Portignon, R.A. Broglia, Phys. Lett. **B 345** (1995) 343.

61. J. Honkanen, V. Koponen, H. Hyvönen, P. Taskinen and J. Äystö, Nucl. Phys. **A 471** (1987) 489.

62. B.H. Wildenthal, M.S. Curtin, and B.A. Brown, Phys. Rev. **C 28** (1983) 1342.

63. M.J.G. Borge, P.G. Hansen, B. Jonson, S. Mattson, G. Nyman, A. Richter, K. Riisager and the ISOLDE collaboration, Z.Phys. **A 332** (1989) 413.

64. E.G. Adelberger, A. Garcia, P.V. Magnus and D.P. Wells, Phys Rev. Lett. **23** (1991) 3658.

65. J.C. Hardy, L.C. Carraz, B. Jonson and P.G. Hansen, Phys. Lett. **B 71** (1977) 307.

J.C. Hardy, B. Jonson and P.G. Hansen, Nucl. Phys. **A 305** (1978) 15.

P.G. Hansen, B. Jonson and A. Richter, Nucl. Phys. **A 518** (1990) 13.

66. B.D. Anderson, A.R. Baldwin, P. Baumann, B.A. Brown, F. Didierjean, C.C. Foster, L.A.C. Carcia, A. Huck, A. Knipper, R. Madey, D.M. Manley, G. Marguier, M. Ramdhane, H. Ravn, C. Richard-Serre, G. Walther and J.C. Watson, Phys. Rev. **C 54** (1996) 602.

67. A. Garcia, E.G. Adelberger, P.V. Magnus, H.E. Swanson, O. Tengblad, ISOLDE collaboration, D.M. Moltz, Phys. Rev. Lett. **67** (1991) 3654.

68. Ari Jokinen, private communication.

69. G. F. Bertsch and H. Esbensen, Rep. Prog. Phys. **50** (1987) 607.

70. M. Oinonen, A. Honkanen, A. Jokinen, T. Siiskonen, J.C. Wang and J. Äystö, JYFL Annual Report 1996, Department of Physics, University of Jyväskylä, Finland (1996) p. 16.

Reprinted from

NUCLEAR INSTRUMENTS & METHODS IN PHYSICS RESEARCH
Section A

Nuclear Instruments and Methods in Physics Research A 395 (1997) 217–225

Gas-silicon detector telescope for charged particle spectroscopy

A. Honkanen[a,*], M. Oinonen[a], K. Eskola[b], A. Jokinen[c,1], J. Äystö[a], The ISOLDE Collaboration

[a]*Department of Physics, Accelerator Laboratory, University of Jyväskylä, FIN-40351 Jyväskylä, Finland*
[b]*Department of Physics, University of Helsinki, FIN-00014 University of Helsinki, Finland*
[c]*PPE Division, CERN, CH-1211 Geneva 23, Switzerland*

Received 11 April 1997

ELSEVIER

Reprinted from

NUCLEAR PHYSICS A

Nuclear Physics A 611 (1996) 47–55

Fine structure in the beta-delayed proton decay of ^{33}Ar

A. Honkanen [a], L. Axelsson [b], J. Äystö [a,c], M.J.G. Borge [d], B. Jonson [b], A. Jokinen [c], I. Martel [d], G. Martínez-Pinedo [e], I. Mukha [f], T. Nilsson [b], G. Nyman [b], B. Petersen [f], A. Poves [e], M.H. Smedberg [b], A. Teijeiro [d], O. Tengblad [c,d]

ISOLDE Collaboration

[a] *Department of Physics, University of Jyväskylä, FIN-40351 Jyväskylä, Finland*
[b] *Fysiska Institutionen, Chalmers Tekniska Högskola, S-412 96 Göteborg, Sweden*
[c] *PPE Division, CERN, CH-1211 Geneva 23, Switzerland*
[d] *Instituto de Estructura de la Materia, CSIC, E-28006 Madrid, Spain*
[e] *Departemento de Fisica Teorica, Universidad Autonoma de Madrid, Cantoblanco, E-28049 Madrid, Spain*
[f] *Institut for Fysik og Astronomi, Aarhus Universitet, DK-8000 Aarhus C, Denmark*

Received 26 July 1996

N·H

ELSEVIER

Reprinted from

NUCLEAR PHYSICS A

Nuclear Physics A 621 (1997) 689–705

High-resolution study of the beta decay of ^{41}Ti ★

A. Honkanen, P. Dendooven, M. Huhta, G. Lhersonneau, P.O. Lipas, M. Oinonen, J.-M. Parmonen, H. Penttilä, K. Peräjärvi, T. Siiskonen, J. Äystö

Department of Physics, University of Jyväskylä, P.O. Box 35, FIN-40351 Jyväskylä, Finland

Received 15 November 1996; revised 14 April 1997

ELSEVIER

PREPRINT No. 1/1998

Beta Decay of ^{31}Ar

L. Axelsson, J. Äystö, M. J. G. Borge, L. M. Fraile, H. O. U. Fynbo, A. Honkanen, P. Hornshoj, A. Jokinen, B. Jonson, P. O. Lipas, I. Martel, I. Mukha, T. Nilsson, G. Nyman, B. Petersen, K. Riisager, M. H. Smedberg, O. Tengblad and ISOLDE Collaboration

Preprint submitted to Elsevier Preprint

Two-proton emission in the decay of ^{31}Ar

L. Axelsson[a], J. Äystö[b,c], U.C. Bergmann[d], M.J.G. Borge[e], L.M. Fraile[e], H.O.U. Fynbo[d], A. Honkanen[b], P. Hornshøj[d], A. Jokinen[c], B. Jonson[a], I. Martel[c,e], I. Mukha[d,1], T. Nilsson[a], G. Nyman[a], B. Petersen[d,2], K. Riisager[d], M.H. Smedberg[a], O. Tengblad[e], ISOLDE Collaboration[c]

[a] *Fysiska Institutionen, Chalmers Tekniska Högskola, S-41296 Göteborg, Sweden*
[b] *Department of Physics, University of Jyväskylä, FIN-40351 Jyväskylä, Finland*
[c] *PPE Division, CERN, CH-1211 Genève 23, Switzerland*
[d] *Institut for Fysik og Astronomi, Aarhus Universitet, DK-8000 Aarhus C, Denmark*
[e] *Instituto Estructura de la Materia, CSIC, E-28006 Madrid, Spain*

Received 15 May 1997; revised 22 October 1997; accepted 28 October 1997

Abstract

Several beta-delayed two-proton branches were observed in the decay of ^{31}Ar, the most intense ones proceeding through the isobaric analogue state (IAS) in ^{31}Cl. The mechanism of the two-proton emission is studied via the energy and angular distributions of the two protons. Simultaneous emission of the two protons fits the present data well, sequential decays might also describe them. Independent of the decay mechanism, a spin of 5/2 for the IAS is suggested. An improved limit on the direct two-proton emission from the ground state of ^{31}Ar is presented.

PACS: 23.40.Hc; 27.30.+t
Keywords: Radioactivity ^{31}Ar(β^+) [from Ca(p,3pxn) reaction]; Measured β-delayed E_p, pp coincidences; ^{31}Ar deduced β2p decay channels; CaO target; surface barrier Si detectors; on-line mass separation

[1] Permanent address: Kurchatov Institute, 123182 Moscow, Russia.
[2] Present address: Dept. of Exp. High Energy Physics, University of Nijmegen, Toernooiveld 1, 6525 ED Nijmegen, The Netherlands.

0375-9474/97/$17.00
PII S0375-9474(97)00623-4